ChemComm

Accepted Manuscript

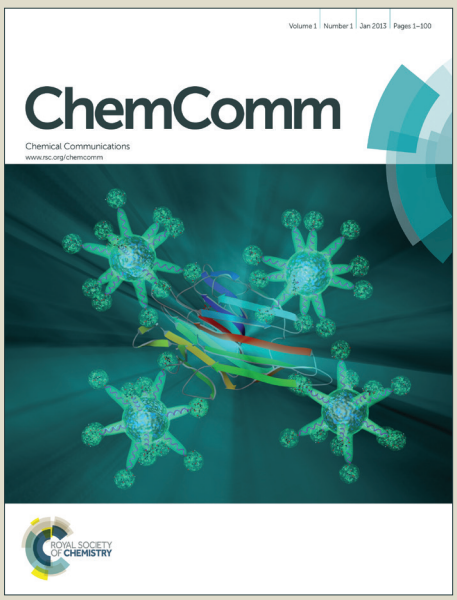

ROYAL SOCIETY OF CHEMISTRY

www.rsc.org/chemcomm

Cite this: DOI: 10.1039/c0xx00000x

www.rsc.org/xxxxxx

Communication

Direct output of electrical signals from LSPR sensors on the basis of plasmon-induced charge separation

Tetsu Tatsuma,* Yu Katagi, Satoshi Watanabe, Kazutaka Akiyoshi, Tokuhisa Kawawaki, Hiroyasu Nishi, and Emiko Kazuma

Received (in XXX, XXX) Xth XXXXXXXXX 20XX, Accepted Xth XXXXXXXXX 20XX
DOI: 10.1039/b000000x

Potentiometric and conductometric sensors based on localized surface plasmon resonance were developed. The sensors can be applied to coloured and turbid samples because light needs not pass through the sample solution.

Propagating surface plasmon resonance (SPR) on a noble metal thin film and localized surface plasmon resonance (LSPR) of a noble metal nanoparticle (NP) are used for biosensing and chemical sensing because changes in refractive index near the metal surface cause resonance angle shifts and resonance wavelength shifts, respectively.[1-3] In general, SPR sensors are more sensitive than LSPR sensors to changes in bulk refractive index, and LSPR sensors could be more sensitive to local refractive index changes just in the vicinity of the metal surface because of their smaller sensing volume.[3] Therefore, if plasmonic NPs are modified with, for instance, antibody molecules, they work as immunosensors. In addition, LSPR sensors are often more cost-effective and suitable for miniaturization, because they require only a simple optical configuration without a prism, which is necessary for SPR sensors. LSPR sensors are therefore suitable for on-site chemical, medical, food and environmental analyses. However, in the LSPR sensing, light passes through the sample solution unlike SPR sensing, in which light is reflected at the back side of the sensor. This often prevents the LSPR sensors from being applied to coloured or turbid sample solutions (Fig. 1a). To address this issue, the sensing is performed at wavelengths at which the sample is relatively transparent (*i.e.*, in spectral windows), by using monodisperse plasmonic metal NPs with a peak in the spectral windows[2] or a LSPR sensor with wavelength-tunable spectral dips.[4] These techniques are, however, not effective if the sample has no spectral window due to broad absorption or high turbidity. We therefore develop novel LSPR sensors in which light need not pass through the sample solution. The sensors exhibit reasonable sensitivities and they can be applied to coloured and turbid sample solutions.

Several years ago, we found plasmon-induced charge separation (PICS) at the plasmonic metal NP-semiconductor interface.[5,6] Since electrons are injected from the plasmonic NPs to semiconductor[5-9] on the basis of external photoelectric effect or hot electron injection, PICS has been widely applied to photovoltaic and photosensing devices,[6,10-15] photocatalysts,[6,16,17] photochromic displays[9,18,19] and photoactuators.[20] Here we exploit PICS for direct output of electrical signals from LSPR sensors. For development of PICS-based LSPR sensors, there are three options for signal transduction: amperometric, potentiometric and conductometric ways. The amperometric sensing is based on redox photocurrent flow due to PICS. In this case, the solution must contain a redox couple and ionic species. The photoexcited metal NPs inject electrons to the semiconductor (n-type)[8] and take electrons from a reduced species in the solution. The electrons injected to the semiconductor are transported to a counter electrode via an external electric circuit and transferred to an oxidized species in the solution.[6] The requirement of the redox species and ionic species make this option less practical. In the case of potentiometric sensing (Fig. 1b),[6] the electron injection

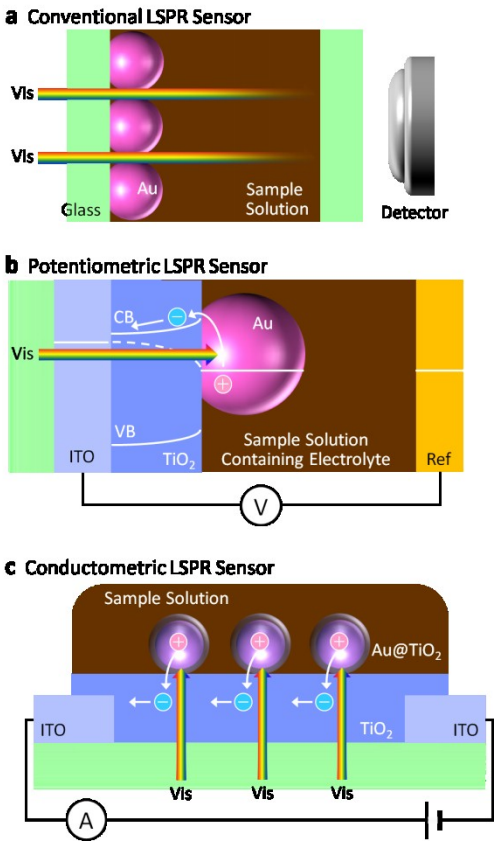

Fig. 1. Mechanisms of the (a) conventional (optical), (b) potentiometric and (c) conductometric LSPR sensors.

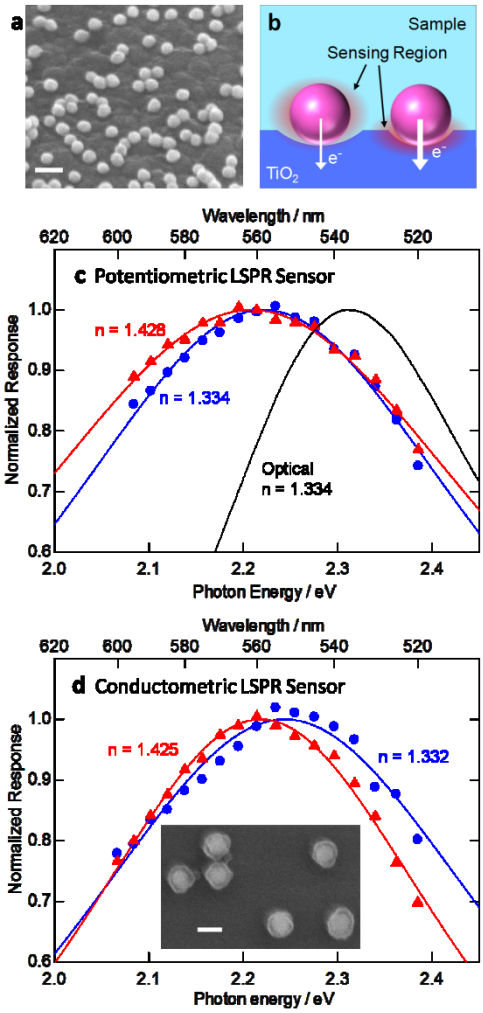

Fig. 2. (a) Scanning electron micrograph of Au NPs on TiO_2 (scale bar = 100 nm). (b) Schematic illustration for Au NPs in poor and good contact with TiO_2. (c) Typical optical and potentiometric spectra of a TiO_2/Au film in water or a water-glycerol mixture. (d) Typical conductometric spectra of a TiO_2/Au@TiO_2 film in water or a water-glycerol mixture. (Inset) Scanning electron micrograph of Au@TiO_2 NPs (scale bar = 50 nm).

from the metal NPs to the semiconductor causes a negative potential shift, which is measured as a signal. Although a reference electrode such as Ag|AgCl is necessary, a redox couple is not necessary because the electron injection need not be continuous. For the same reason, the electrolyte concentration could be low. In the case of conductometric sensing (Fig. 1c), a couple of electrodes are interconnected with a semiconductor film or wire modified with plasmonic NPs. The electron injection from the excited NPs to the conduction band of the semiconductor increases its conductivity.[12-14] If a bias voltage is applied between the two electrodes, an electric current flows between them. The current depends on the rate of the electron injection. The sample can be a small amount of liquid, which is not necessarily ionically conductive.

Thus, we developed a potentiometric and conductometric LSPR sensors in this work. An electrode for potentiometric sensing was fabricated as follows. A TiO_2 film (~70 nm thick) was prepared on an ITO-coated glass plate by a spray pyrolysis method (0.12 MPa, 1 s for 4 times, 450 °C) from 2-propanol containing 0.028 M titanium diisopropoxide bis(acetylacetonate) (TDBA) followed by annealing at 450 °C for 30 min. Citrate-protected Au NPs (40 nm, Tanaka Kikinzoku) were adsorbed onto the TiO_2 surface by immersing the substrate in an Au NP dispersion at pH 2.7 for 6 h. The surface density of the adsorbed Au NPs was 77.0 ± 4.4 particles μm^{-2} (mean ± standard error). The electrode surface had the nanoscale roughness, and most Au NPs were located at the dents at the electrode surface (Fig. 2a).

Open-circuit potential of the ITO/TiO_2/Au NP electrode was measured in water (refractive index n = 1.33) in reference to a Ag|AgCl electrode with a potentiostat. A negative potential shift was observed when the electrode was irradiated from the backside with visible light (full width at half maximum = 20 nm, 5×10^{15} photons cm^{-2} s^{-1}) using an opto-spectrum generator (Hamamatsu Photonics). In Fig. 2c, typical potential shifts -ΔE at t = 60 s (light irradiation was started at t = 0 s) are plotted against the energy of irradiated photons. The photopotential action spectrum thus obtained shows a peak at 557.8 ± 1.4 nm (for three independently prepared electrodes), which is not observed for an ITO/TiO_2 electrode without Au NPs. The peak wavelengths were evaluated by Lorentzian fitting. The negative potential shift is explained in terms of the electron injection from photoexcited Au NPs to the TiO_2 conduction band due to PICS.[6,8]

On the other hand, the extinction (= absorption + scattering) spectrum of the Au NPs loaded on the TiO_2 film is peaked at 534.3 ± 1.76 nm in water (Fig. 2c). The redshift of the photopotential peak could reflect that the NPs in better contact with TiO_2, which exhibit redshifted peaks because of high refractive index of anatase TiO_2 (~2.5 at 550 nm), make a better contribution to PICS because the good contact facilitates the electron transfer (Fig. 2b). The photopotentiometric peak was broader than that of the optical peak, because of the saturation of the potential shifts.

The photopotential responses can be obtained even in a water-glycerol mixture, which has higher refractive index (n = 1.43) as shown in Fig. 2c. The peak is redshifted as the refractive index increases. We examined dependence of the photopotential peak wavelength on the refractive index of sample liquids by using water-glycerol mixtures with different refractive indices (Fig. 3a). The slope of the plot, namely the refractive index sensitivity of the potentiometric LSPR sensor, is 33.2 ± 4.2 nm RIU^{-1}. In comparison with the sensitivity of the optical sensing based on the extinction peak shift, 44.6 ± 6.3 nm RIU^{-1}, the sensitivity of the potentiometric sensor is lowered by ~26%. It is known that plasmonic electron oscillation of a NP on a solid substrate is localized at the NP-substrate interface when the contact area is large and the refractive index of the substrate is high.[21,22] Therefore, NPs in good contact with TiO_2, which make significant contribution to the potentiometric responses as described above, have suppressed sensitivities because a large portion of their sensing region is occupied by TiO_2 (Fig. 2b).

Next we developed a conductometric sensor (Fig. 1c). Here we used Au@TiO_2 NPs to avoid direct electrical contact between Au NPs, which could unduly lower the film conductivity. Au@TiO_2 core-shell NPs were synthesized as follows.[23] In short, Au NP dispersion (40 nm, 10 mL) was mixed with 0.5 wt% hydroxypropyl cellulose (400 μL) and stirred for 20 h. This

solution (2.5 mL) was mixed with 2-propanol (10 mL), followed by successive addition of 28% ammonia (312 μL) and 2-propanol containing 10 mM TDBA (20 μL). The mixture was stirred for 20 h. The obtained Au@TiO_2 NPs were centrifuged at 8000*g* for 40 min and suspended in 2-propanol. Scanning electron micrograph of the synthesized Au@TiO_2 NPs is shown in Fig. 2d (inset). Au cores are covered with 5−7-nm-thick TiO_2 shells.

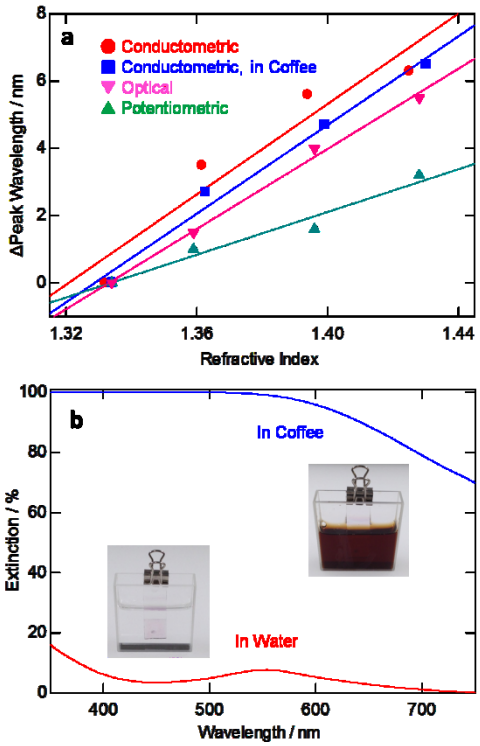

Fig. 3. (a) Typical optical and potentiometric responses of a TiO_2/Au film and conductometric responses of a TiO_2/Au@TiO_2 film to refractive index changes. (b) Extinction spectra and photographs (insets) of a TiO_2/Au@TiO_2 film in water or coffee.

An ITO film (200 nm thick) on a glass plate (12 × 40 mm) was partially etched by aqua regia so that it was divided into two electrodes separated with a 2-mm gap. The gap (bare glass) was coated with a TiO_2 thin film (~60 nm thick) by the spray pyrolysis method (1 s for 2 times) from 2-propanol containing 0.11 M TDBA. The Au@TiO_2 NPs were adsorbed onto the TiO_2 and annealed at 500 °C for 30 min. The surface density of the adsorbed Au@TiO_2 NPs was about 86 particles μm^{-2}.

Pure water was loaded onto the gap region (~20 μL) and a bias dc voltage of 1 V was applied between the electrodes. Lateral dc conductivity of the film was measured under visible light (7×10^{15} photons cm^{-2} s^{-1}) from the opto-spectrum generator. Figure 2d shows a typical conductivity action spectrum of the TiO_2/Au@TiO_2 film in water. The peak at 556.4 ± 1.9 nm is, again, ascribed to LSPR, since it is not observed for a conductometric device without plasmonic NPs. Note that ac voltage should not be applied because ac currents would flow in a solution and the measured conductivity could reflect that of the solution rather than the film.

The photoconductivity peak is also redshifted as the refractive index of the sample liquid increases (Fig. 2d). The plot of the peak wavelength evaluated on the basis of the Lorentzian fitting is shown in Fig. 3a as a function of the refractive index. The refractive index sensitivity of the conductometric LSPR sensor, 64.7 ± 6.7 nm RIU^{-1}, is close to that of the optical sensing with the TiO_2/Au@TiO_2 film, 62.9 nm RIU^{-1}, probably because all of the Au cores are in good contact with the TiO_2 shell and almost equally contribute to the conductometric responses. The sensitivities of the TiO_2/Au@TiO_2 film are significantly higher than that of the potentiometric LSPR sensor with the TiO_2 film modified with bare Au NPs. As described above, the sensitivity of the potentiometric sensor is suppressed because the electron oscillation is localized at the NP-TiO_2 interface and the sensing region is substantially occupied by TiO_2. On the other hand, in the case of the Au@TiO_2 NPs adsorbed on TiO_2, the electron oscillation is delocalized over the whole NP surface because the Au core is covered with the TiO_2 shell, and therefore the masking by the TiO_2 substrate is less significant. Actually, potentiometric sensing with an ITO/TiO_2/Au@TiO_2 electrode showed the sensitivity of ~70 nm RIU^{-1}.

The conductometric LSPR sensor was applied to a coloured and turbid sample liquid. Here we tested canned black coffee as a sample. The LSPR peak of the Au@TiO_2 NPs on the TiO_2 film is not obvious in the extinction spectrum in the coffee sample (Fig. 3b). However, the conductivity action spectrum clearly shows an LSPR peak and its refractive index sensitivity for coffee containing glycerol, 65.9 nm RIU^{-1}, is in good agreement with that in transparent solutions. Thus, the present sensor can be applied to sample solutions with no significant spectral windows.

Conclusions

Potentiometric and conductometric LSPR sensors were developed in the present work. Both of them output electrical signals directly from the LSPR sensor and therefore require no extra photodetector. Since light needs not pass through a sample solution, the sensors can be applied to coloured and turbid samples.

Acknowledgements

This work was supported in part by a Grant-in-Aid for Scientific Research No. 25288063 and a Grant-in-Aid for Challenging Exploratory Research No. 25600002.

Notes and references

[a] *Institute of Industrial Science, University of Tokyo, 4-6-1 Komaba, Meguro-ku, Tokyo 153-8505, Japan. E-mail: tatsuma@iis.u-tokyo.ac.jp*

1 J. Homola, *Chem. Rev.*, 2008, **108**, 462.
2 K. M. Mayer and J. H. Hafner, *Chem. Rev.*, 2011, **111**, 3828.
3 A. G. Brolo, *Nat. Photonics*, 2012, **6**, 709.
4 E. Kazuma and T. Tatsuma, *Nanoscale*, 2014, **6**, 2397.
5. Y. Tian and T. Tatsuma, *Chem. Commun.*, 2004, 1810.
6. Y. Tian and T. Tatsuma, *J. Am. Chem. Soc.*, 2005, **127**, 7632.
7. N. Sakai, Y. Fujikawa, Y. Takahashi and T. Tatasuma, *ChemPhysChem*, 2009, **10**, 766.
8. E. Kazuma and T. Tatsuma, *Adv. Mater. Interfaces*, 2014, **1**, 1400066.
9. T. Tatsuma, *Bull. Chem. Soc. Jpn.*, 2013, **86**, 1.
10. Y. Takahashi and T. Tatsuma, *Appl. Phys. Lett.*, 2011, **99**, 182110.
11. M. W. Knight, H. Sobhani, P. Nordlander and N. J. Halas, *Science*, 2011, **332**, 702.
12. M.-S. Son, J.-E. Im, K.-K. Wang, S.-L. Oh, Y.-R. Kim and K.-H. Yoo, *Appl. Phys. Lett.*, 2010, **96**, 023115.

13. S. Mubeen, G. Hernandez-Sosa, D. Moses and J. Lee, M. Moskovits, *Nano Lett.*, 2011, **11**, 5548.
14. F. Wu, L. Tian, R. Kanjolia, S. Singamaneni and P. Banerjee, *ACS Appl. Mater. Interfaces*, 2013, **5**, 7693.
15. P. Reineck, G. P. Lee, D. Brick, M. Karg and P. Mulvaney, *Adv. Mater.*, 2012, **24**, 4750.
16. E. Kowalska, R. Abe and B. Ohtani, *Chem. Commun.*, 2009, 241.
17. A. Tanaka, K. Hashimoto and H. Kominami, *J. Am. Chem. Soc.*, 2012, **134**, 14526.
18. Y. Ohko, T. Tatsuma, T. Fujii, K. Naoi, C. Niwa, Y. Kubota and A. Fujishima, *Nature Mater.*, 2003, **2**, 29.
19. E. Kazuma and T. Tatsuma, *Chem. Commun.*, 2012, **48**, 1733.
20. T. Tatsuma, K. Takada and T. Miyazaki, *Adv. Mater.*, 2007, **19**, 1249.
21. L. J. Sherry, S.-H. Chang, G. C. Schatz, R. P. Van Duyne, B. J. Wiley, and Y. Xia, *Nano Lett.*, 2005, **5**, 2034.
22. I. Tanabe and T. Tatsuma, *Nano Lett.*, 2012, **12**, 5418.
23. Z. W. Seh, S. Liu, S.-Y. Zhang, M. S. Bharathi, H. Ramanarayan, M. Low, K. W. Shah, Y.-W. Zhang and M.-Y. Han, *Angew. Chem.*, 2011, **123**, 10322.